

# Inhibition of Peripheral ERK Signaling Ameliorates Persistent Muscle Pain Around Trigger Points in Rats

Cell Transplantation  
Volume 29: 1–12  
© The Author(s) 2020  
Article reuse guidelines:  
sagepub.com/journals-permissions  
DOI: 10.1177/0963689720960190  
journals.sagepub.com/home/cll  


Yu-Chang Zhu<sup>1,2</sup> , Fei-Hong Jin<sup>1</sup>, Ming-Yang Zhang<sup>3</sup>,  
and Feng Qi<sup>1</sup>

## Abstract

The purpose of this study was to investigate whether the ERK signaling pathway was involved in ameliorating chronic myofascial hyperalgesia from contused gastrocnemius muscle in rats. We established an animal model associated with myofascial pain syndrome and described the mechanism of muscle pain in an animal model. Changes in the mechanical pain threshold were observed 0.5, 1, 2, 3, 4, 5, 8, 12, 18, and 24 h after ERK inhibitor injection around myofascial trigger points (MTrPs) of the gastrocnemius muscle in rats. Morphological changes in gastrocnemius muscle cells were observed by hematoxylin and eosin (H&E) staining. ERK signaling pathway activation was detected through immunohistochemistry and Western blotting. The main morphological characteristics of injured muscle fibers around MTrPs include gathered circular or elliptical shapes of different sizes in the cross-section and continuous inflated and tapering fibers in the longitudinal section. After intramuscular injection of U0126 (ERK inhibitor), the mechanical pain threshold significantly increased. The reduction in mechanical hyperalgesia was accompanied by reduced ERK protein phosphorylation, myosin light chain kinase (MLCK) protein, p-MLC protein expression, and the cross-sectional area of skeletal muscle cells around MTrPs. An ERK inhibitor contributed to the attenuation of mechanical hyperalgesia in the rat myofascial pain model, and the increase in pain threshold may be related to MLCK downregulation and other related contraction-associated proteins by ERK.

## Keywords

ERK, MLCK, myofascial pain syndrome, trigger point, gastrocnemius muscle

## Introduction

Chronic pain can weaken the body, affects more than one-fifth of the world's population, and is among the most disabling and costly afflictions<sup>1,2</sup>. Myofascial pain syndrome (MPS) is a general chronic pain disorder characterized by the existence of one or more myofascial trigger points (MTrPs) in the corresponding myofascial sites of patients. The signature feature of MTrPs is a hard, taut band (TB), which consists of a group of contracted muscle fibers that can be palpated in the muscle and are characterized by distant referred pain, local twitch responses (LTRs), and spontaneous electrical activity<sup>3</sup>. MTrPs can be clinically classified as latent or active<sup>4</sup>. A clinical survey revealed that 40% of musculoskeletal symptoms occur secondary to pain caused by active MTrPs<sup>3</sup>. MTrPs are thought to occur as a result of muscle strain or injury or psychological stress. Imbalances in human mechanics, incorrect posture, prolonged muscle contraction, and muscle atrophy are associated with the development of MTrPs<sup>5</sup>. Observations of the muscle

histomorphology of MTrPs in patients with MPS revealed that some large and small hyperchromatic rounded muscle cells appeared in the transection of the tissue<sup>6</sup>. Some large rounded fibers were found in transverse sections of MTrP muscle tissue, and some muscle fibers were found in the

<sup>1</sup> Department of Anaesthesiology and Pain Clinic, Qilu Hospital, Cheeloo College of Medicine, Shandong University, Jinan, Shandong, China

<sup>2</sup> Department of Anaesthesiology, Shandong Provincial Maternal and Child Health Care Hospital, China

<sup>3</sup> Department of Anaesthesiology, Tengzhou Central People's Hospital, Tengzhou, Shandong, China

Submitted: May 6, 2019. Revised: August 28, 2020. Accepted: August 31, 2020.

## Corresponding Author:

Feng Qi, Department of Anaesthesiology and Pain Clinic, Qilu Hospital, Cheeloo College of Medicine, Shandong University, No. 107 Wenhua Road, Jinan, Shandong 250012, China.  
Email: qifeng66321@sina.com



longitudinal sections with central bulges and narrowing and lengthening on both sides. These characteristics may be specific histological markers of MTrPs<sup>7</sup>, as subsequently confirmed by researchers in animal models of MPS<sup>8</sup>. Although injured muscle fibers were found around the MTrPs, the mechanism of chronic muscle pain remains unclear, hindering the development of appropriate analgesic strategies.

Reports on the biological mechanism of myofascial triggers in humans and rats are limited, and most of them have been studied to evaluate the effect of clinical therapy. Recently, in the same model as that used in this study, inflammatory cytokine expression levels were significantly increased in the MTrPs of the model group<sup>9</sup>, and Huang and colleagues used this model to study proteomics, providing valuable clues for improved understanding of the pathogenesis of myofascial pain<sup>10</sup>. A sustained increase in acetylcholine in the synaptic cleft may play a key role in MTrP formation<sup>11</sup>.

Small foci of contracted sarcomeres have been found in the human trapezius, which is consistent with the hypothesis of MTrP formation<sup>12</sup>. Studies have demonstrated the presence of sympathetic hyperactivity at MTrPs, which could partially explain its symptoms<sup>13</sup>. Part of our previous studies demonstrated that the fibroblast growth factor receptor (FGFR1) sensitizes nociceptive nerves around MTrPs and mediates pain behaviors in rats<sup>14</sup>. At present, the diagnosis of MTrPs is based exclusively on clinical examination<sup>10</sup>.

A large body of evidence suggests that the mitogen-activated protein kinase (MAPK) pathway plays a key role in the formation of peripheral and central sensitization through different molecular and cellular mechanisms to promote hypersensitivity to pain after tissue and nerve damage<sup>15,16</sup>. MAPK signal cascades are activated by many intracellular and extracellular stimuli, including hypoxia, changes in the Ca<sup>2+</sup> concentration, physical pressure, and cytokines<sup>17</sup>. The extracellular signal-regulated kinase (ERK1/2) signaling pathway in animal cells is the most commonly activated pathway among the MAPK pathways<sup>18</sup>. Through studies of different pain models, peripheral or central noxious stimuli were found to abnormally stimulate the ERK1/2 signaling pathway in the nervous system, and activated ERK1/2 plays a vital role in the formation and maintenance of pain hypersensitivity<sup>16,19</sup>. In addition, ERK is involved in cell contraction through the myosin light chain kinase (MLCK) signaling pathway<sup>20,21</sup>. MLCK induces myosin regulatory light chain (RLC) phosphorylation, which regulates the contraction of smooth muscle, skeletal muscle, and cardiomyocytes. Skeletal muscle expresses a specific MLCK called skeletal muscle type myosin light chain kinase (skMLCK), which has a vital function in skeletal muscle contraction.

SkMLCK is a specific Ca<sup>2+</sup>/calmodulin-dependent protein kinase that phosphorylates the RLC of sarcomeric myosin<sup>22</sup>. Phosphorylation of RLC in skeletal muscle increases the isometric contraction force of muscle fibers, the rate of the production of the submaximum and maximum levels of

**Table 1.** The Number of Animals in Each Group.

Group	Behavioral testing	H&E/IHC	WB
Control	6	3	6
MPS + DMSO	6	3	6
MPS + U0.2	6	3	6
MPS + UI	6	3	6

DMSO: dimethyl sulfoxide; H&E: hematoxylin and eosin; IHC: Immunohistochemistry; WB: Western blot.

force when Ca<sup>2+</sup> induces muscle contraction<sup>23</sup>. By increasing the calcium sensitivity of skeletal muscle fibers through the above described mechanism, this effect may enhance the ability of sarcomeres to contract, thereby affecting dynamic aspects of overall muscle performance<sup>24</sup>. Therefore, abnormal expression of RLC may lead to changes in muscle contractility. The maximum muscle strength of phosphorylated RLC skinned fibers was increased by 15% compared to that of reconstituted, nonphosphorylated RLC skinned fibers<sup>25</sup>. Abnormal changes in MLCK may lead to abnormal muscle contractions and even muscle damage. When the skMLCK gene was knocked out in mice, electrical stimulation of skeletal muscle in mice did not result in phosphorylation of RLC and was accompanied by a decreased muscular tetanic contraction potential caused by spasmodic toxin and a significantly decreased staircase effect<sup>26</sup>. The role of skMLCK in regulating skeletal muscle contraction, as demonstrated here and earlier by others, may be more important than was first suspected or realized.

In this study, to better study the pathogenesis mechanism of MPS, we attempted to establish an animal model simulating MPS, which is characterized by the presence of injured muscle fibers accompanied by persistent muscle pain. We examined the histological changes around MTrPs and the role of the ERK signaling pathway in persistent muscle pain from contused gastrocnemius muscle in rats.

## Materials and Methods

### Animal Care and Experimental Protocol

The research procedures were authorized by the Animal Care and Use Committee of Shandong University. The rats required for the experiment were all maintained in accordance with the "Guidelines for Animal Care and Use in the Laboratory of Shandong University, People's Republic of China." Six-week-old male Sprague-Dawley (SD) rats (200–250 g) were housed in groups of three under a 12-h light/dark cycle. To reduce experimental error, all the behavioral tests and tissue separation were performed by the same person, and other related procedures, such as drug injection, were performed by another experimenter. This experiment adopted a double-blind method. In our experiment, animals were randomly divided into different groups as indicated in Table 1, and the protocol of the experiment is shown in Fig. 1.

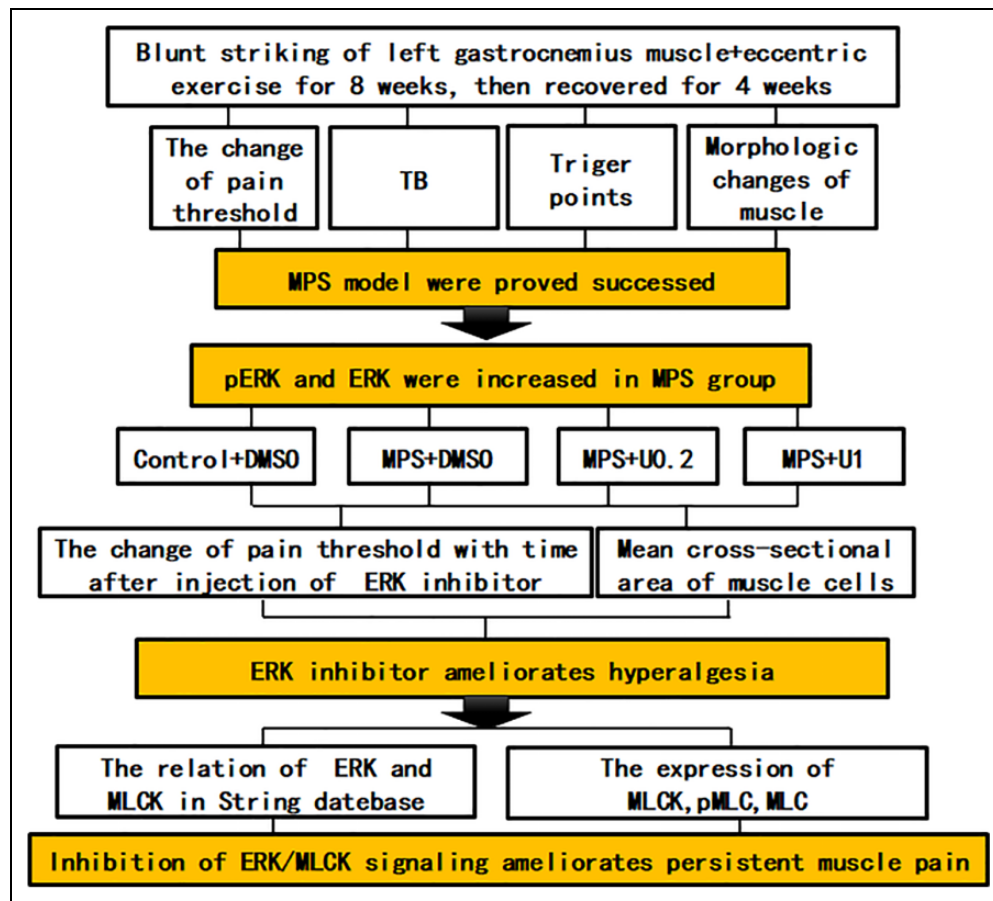


**Figure 1.** The flow chart of the experiment.

### Animal Modeling

In this study, we used the same animal model as that reported by Zhang et al<sup>8</sup>. Rats were randomly divided into four groups using a web-based random number generator (GraphPad software): control group, MPS + dimethyl sulfoxide (DMSO) group, MPS + U0.2 group, and MPS + U1 group. The model of MTrP activation in rats was established by blunt striking of the left gastrocnemius muscle combined with eccentric exercise for 8 weeks followed by a 4-week recovery period. Rats were briefly anesthetized with 2.5% isoflurane and fixed under the striking device. The site of the left gastrocnemius muscle was marked, and then the stick fell 20 cm freely to strike the marked position with a kinetic energy of 2.352 J once each week on the first day of the week. After each blow, the skin and bone were verified to be intact, and the rats were fed normally. Every second day of each week, the rats were run on the running platform (Sans, Nanjing, China) at an angle of  $-16^\circ$ , and the speed was gradually increased to 16 m/min over 90 min. The general health of the rats during the procedures, such as body weight, condition of the limbs, and movement ability, was monitored weekly. To identify the active MTrPs, we first palpated and marked the contracture nodule

in the TB. If it was found that acupuncture could cause a LTR, the labeled nodules were considered as possible active MTrPs. Second, the mechanical sensitivity to TB was significantly decreased as further confirmed.

### TB Palpation

An obvious tight rope structure felt in the muscle is known as a TB, and the presence of a TB was examined using the flat palpation method described by Huang et al<sup>3</sup>. In brief, the evaluator palpated the subcutaneous muscle tissue of the rat gastrocnemius muscle with a fingertip and considered it a TB if there was a prominent tubercle-like cord in the muscle fibers rolling under the skin. During the modeling period, the left gastrocnemius muscle of the rat was palpated on the last day of each week to determine the presence of a TB.

### Behavioral Testing

Mechanical stimulation was used to determine the withdrawal threshold of the lower limbs to evaluate the mechanical hyperalgesia of rats. Briefly, we used the Randall-Selitto instrument (Shandong Provincial Institute

of Science and Technology, Jinan, China), which has a round head probe (tip diameter: 8 mm)<sup>27,28</sup>. Before the behavioral test, all rats were acclimated to the laboratory environment for 7 days to reduce errors caused by the environment. In addition, we also conducted behavioral adaptation experiments during the adaptation period. During the measurements, the rats were confined to a cylinder with their lower limbs exposed. In the measurement with the Randall-Selitto instrument, the probe continuously pressed the left gastrocnemius muscle of the rat until the limb retracted. Each rat was measured seven times at 2-min intervals. The maximum and minimum values were removed, and the average value of the remaining values was taken as the initial value of the withdrawal threshold. A Randal-Selitto device was used to determine the mechanical withdrawal threshold at 0.5, 1, 2, 3, 4, 5, 8, 12, 18, and 24 h after intramuscular injection of U0126. The blind method was used in the behavioral test.

### *Injection of ERK Inhibitor*

After successful modeling, the effect of the MAPK kinase (MEK) inhibitor U0126 (MCE) on the withdrawal threshold of the left lower limb in rats stimulated by mechanical pressure was studied at week 13. The diagnostic criteria for active MTrPs were as follows: (1) tender spot in a palpable TB, (2) elicitation of a LTR by palpation or needle insertion into the tender spot, and (3) significantly decreased mechanical withdrawal threshold of the TB in the gastrocnemius. Specifically, if LTR was elicited by needling, the marked nodule was considered a possible active MTrP. The skin overlying the TB was disinfected with alcohol. Immediately after the intramuscular injection of the drug, a thin, indelible ink pen was used to mark the punctured part of the skin such that the mechanical withdrawal threshold of the intramuscular injection site could be repeatedly measured. The ERK inhibitor which was dissolved with 1% DMSO (0.2 and 1 µg/µl concentrations) (30 µl/point) was intramuscularly administered to the MTrPs (one to three points), and the effect of the vehicle (1% DMSO) was also tested at the same volume as that used for the inhibitor in MTrPs or control animals (one to three points).

### *Hematoxylin and Eosin Staining*

One hour after the TB sites were injected with the drug, muscle samples around active MTrPs were collected along the pinholes in the skin marked with a fine-tip indelible ink pen. The muscle biopsy samples were fixed with formalin, embedded in paraffin, and sectioned. The samples were sliced at a thickness of 3 µm, placed on the slide, and stained with hematoxylin and eosin (H&E). The slices were then dehydrated in graded ethanol (70%–100%) and xylene and covered. All slices were evaluated using an optical microscope with a digital camera.

### *Immunohistochemistry*

We performed histomorphological identification of highly suspected MTrPs by H&E staining to further determine the accuracy of the sampling location. Typical morphological characteristics of MTrPs include gathered circular or elliptical shape with different sizes within the cross-section and continuous inflated and tapering fibers within the longitudinal section. If the muscle tissue of the sampling site conformed to active MTrP morphology, the remaining tissue sections were used for immunohistochemistry (IHC). IHC was used to label tissues with streptavidin–biotin. Paraffin-embedded sections were heated at 68°C for 2 h and then deparaffinized. The sections were subjected to microwave irradiation with ethylenediaminetetraacetic acid buffer (pH 8) for 15 min. After rinsing twice in phosphate buffered saline (PBS), the slices were incubated in 3% hydrogen peroxide. After washing in PBS thrice, the sections were treated with normal goat serum at 37°C for 30 min followed by incubation with ERK antibody (1:200, ab17942, Abcam, Cambridge, UK) and primary polyclonal rabbit anti-pERK1/2 antibody (1:400, #4370, CST, Boston, MA, USA) at 4°C overnight. After washing in PBS thrice, the slices were incubated with biotin-labeled goat antirabbit serum at 37°C for 30 min and horseradish peroxidase labeled streptavidin complex at 37°C for 30 min (Origene sp-9000). DAB matrix solution and hematoxylin were used for color development. The images were obtained with a BX53 microscope (Olympus, Tokyo, Japan) using a QImaging Micropublisher camera (Abingdon, Virginia, USA).

### *Western Blot Analysis*

The method of muscle tissue harvesting was described above. Tissue samples were quickly frozen in liquid nitrogen for later use in the Western blot (WB) experiments. Muscle tissue was ground in a liquid nitrogen environment and then subjected to violent shock in precooled lysis buffer. The supernatant was collected after centrifugation, and the protein concentration was determined. The samples of total protein were separated by 5% and 10% sodium dodecyl sulfate polyacrylamide gel electrophoresis. The proteins were then transferred to polyvinylidene fluoride membranes. The membranes were incubated at room temperature in 5% milk for 1 h. Then, the membranes were incubated overnight with primary antibody at 4°C followed by secondary antibodies for 1 h. The primary antibodies used in this experiment were as follows: rabbit anti-ERK polyclonal antibody (1:1,000, ab17942, Abcam), rabbit anti-pERK1/2 polyclonal antibody (1:2,000, #4370, CST), rabbit anti-MLCK polyclonal antibody (1:1,000, DF9023, Affinity Biosciences, Changzhou, China), rabbit anti-MLC2 polyclonal antibody (1:1,000, DF7911, Affinity Biosciences, Changzhou, China), rabbit anti-p-MLC2 (Ser15) polyclonal antibody (1:1,000, AF8618, Affinity Biosciences, Changzhou, China), and goat anti-rabbit antibody as the secondary

antibody (1:5,000, Zhongshan Golden Bridge, Beijing, China). The protein bands were visualized with a Fluoro-Chem 9900 Imaging System, and the expression of target protein was quantified by comparing it with the expression of glyceraldehyde 3-phosphate dehydrogenase (1:1,000, ProteinTech, Wuhan, China).

### Measurement of Cross-sectional Area

Three rats in each group were used for H&E/IHC. We randomly selected one H&E section from each rat and then randomly selected three microscope fields ( $\times 400$ ). The cross-sectional area of entire fibers in this field was measured and averaged.

### Predicting the Relationship Between ERK and MLCK

To further confirm the underlying mechanism of the ameliorating effect of ERK inhibitor on persistent muscle pain associated with TB, we searched for the proteins associated with ERK that were related to muscle contraction in the STRING database (<https://string-db.org/cgi/input.pl>). Then, the related protein was assessed.

### Statistical Analyses

Statistical analyses were performed using SPSS 19.0 software (IBM, Armonk, NY, USA). All data are expressed as the means  $\pm$  standard error of the mean (SEM). The comparison between the two groups was analyzed by the *T*-test. When there were at least three groups, the data were analyzed using one-way analysis of variance to determine the within-group values. Fisher's Least Significant Difference post hoc tests were conducted when appropriate. Statistical significance was defined as  $P < 0.05$ ,  $*P < 0.05$ , and  $**P < 0.01$ .

## Results

### Mechanical Pain Threshold Changes, Number of MTrPs, and Histomorphological Changes

To investigate the mechanisms underlying myofascial pain, we established an MPS model in SD rats. The changes in the mechanical withdrawal threshold of the left lower limb gastrocnemius muscle in rats were measured using a Randall-Selitto device every week. No abnormal limb lifting, foot licking, gait instability, or other pain-related behaviors were observed in the control group. Two weeks after the first strike, compared with that in the control group, the mechanical withdrawal threshold in the MPS group was significantly decreased, persisting until the 12th week of the modeling cycle ( $**P < 0.01$ ) (Fig. 2A). The subcutaneous longitudinal cord palpated in the middle of the gastrocnemius muscle was a TB. No TB was detected by palpation in the control group. TBs were first palpated at 2 weeks, and the proportion of palpable TBs reached 100% starting at 5 weeks and continuing through 12 weeks of the

modeling cycle (Fig. 2B). After successful modeling, enlarged nodules could be found when palpating the gastrocnemius muscle in the MPS group, and acupuncture of the nodules could induce LTRs. The number of MTrPs was determined according to the LTRs. Compared with that in the control group, the number of MTrPs was increased significantly in the MPS group (Fig. 2C). After H&E staining, we first used a low-power microscope ( $\times 100$ ) to display the morphological characteristics of the transverse sections of the two groups of muscle fibers on the whole. At high magnification ( $\times 400$ ), we found that the muscle fibers were uniform in size, polygonal, and regular in arrangement in the cross-sectional space in the control group (arrows). The muscle fibers in the MPS group were annular or elliptical hyperchromatic muscle fibers of different sizes (arrows). The abnormal fibers aggregated together, and minimal inflammatory cells were observed (Fig. 2D). In the longitudinal sections of muscle, the muscle cells were tightly ordered in the control group. Continuous expansion of pyramidal muscle fibers was found in the MPS group. The muscle fiber space was increased, and obvious inflammatory cell infiltration was observed in the MPS group (Fig. 2E).

### ERK and p-ERK Expressions were Increased in Injured Muscle Fibers Around MTrPs of the Gastrocnemius Muscle of SD Rats

We found that ERK and p-ERK were significantly increased in injured muscle fibers around MTrPs of the gastrocnemius muscle of SD rats. As demonstrated by immunohistochemical staining, ERK was increased in the cytoplasm of large or small rounded muscle cells (arrows), and p-ERK was increased in the cell nuclei of muscle cells (arrows) in the MPS group (Fig. 3A). WB results revealed that ERK protein and p-ERK protein expression were significantly increased in injured muscle fibers around MTrPs in the MPS group compared with those in the control group (Fig. 3B, C). The mean cross-sectional area of the injured muscle fibers in the MPS (with ERK immunohistochemical staining of positive cells) group was significantly increased compared with that in the control group and the MPS (no ERK immunohistochemical staining of positive cells) group (Fig. 3D). The mean cross-sectional area of the injured muscle fibers in the MPS (with p-ERK immunohistochemical staining of positive cells) group was significantly increased compared with that in the control group and the MPS (no p-ERK immunohistochemical staining of positive cells) group (Fig. 3E).

### ERK Inhibitor Restrained the Expression of p-ERK in Injured Muscle Fibers Around MTrPs

To investigate the effect of ERK in mechanical hyperalgesia, we injected two different concentrations (0.2 and 1  $\mu\text{g}/\mu\text{l}$ ) of the ERK inhibitor U0126 into the gastrocnemius muscle of SD rats. One hour after injection, we performed western

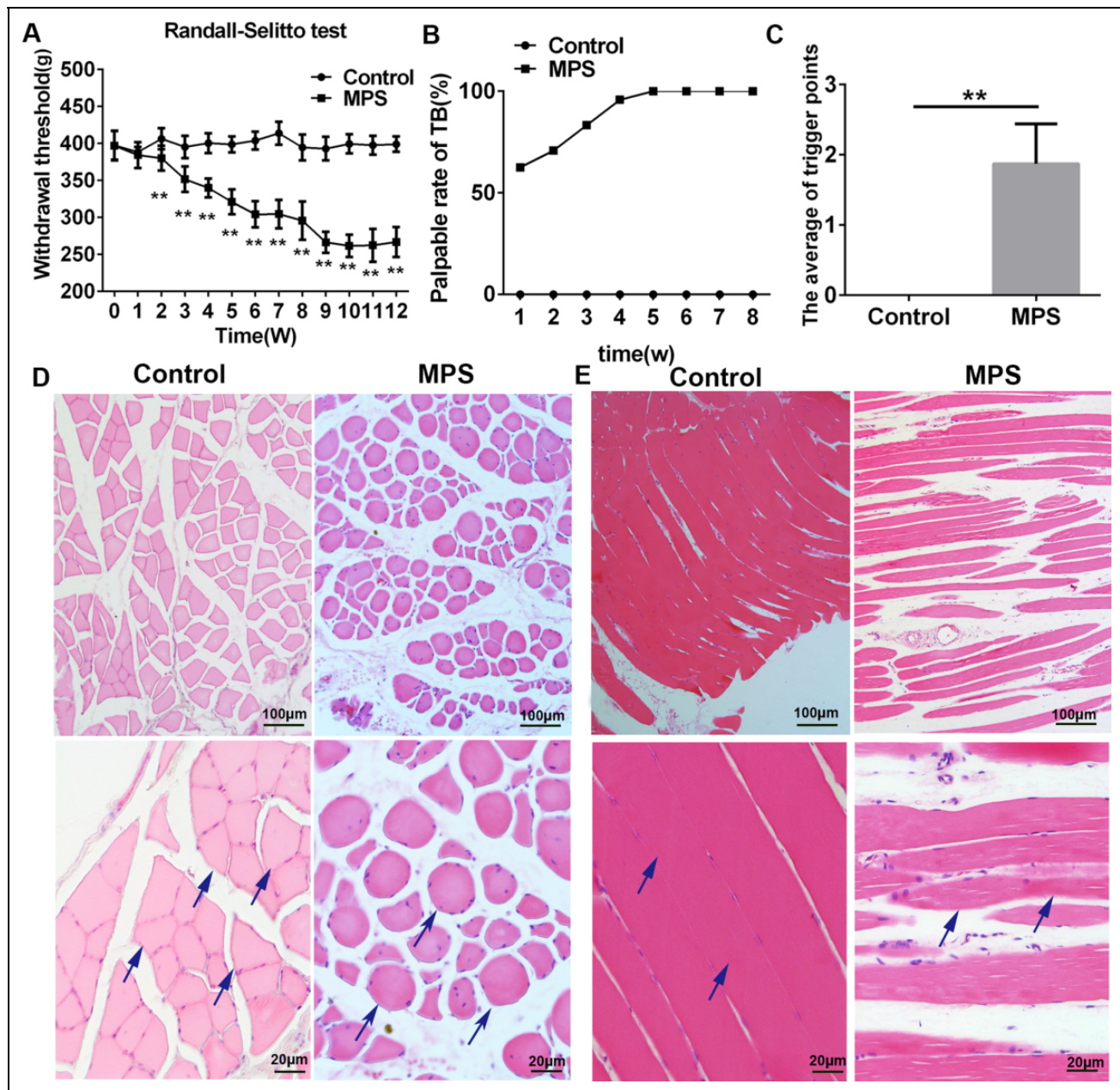


**Figure 2.** The MPS model was successfully generated. (A) Weekly changes in the mechanical withdrawal thresholds measured by the Randall-Selitto apparatus in the left gastrocnemius muscle of rats. Data are presented as the mean  $\pm$  SEM ( $n = 6$ ). The data were analyzed by *T*-tests.  $*P < 0.05$ ,  $**P < 0.01$ . (B) The proportion of nodules in the left gastrocnemius muscle in each group measured on a weekly basis. In the model group, the palpable rate of the TBs reached 100% by the fifth week of the modeling cycle. (C) After modeling, the average number of MTRPs in the two groups is shown. Data are presented as the mean  $\pm$  SEM ( $n = 6$ ). The data were analyzed by *T*-tests.  $*P < 0.05$ ,  $**P < 0.01$ . (D) Light microscopy images of cross-sections of muscle fibers with H&E staining. In the control group, the muscle cells showed polygonal shapes of uniform size (arrows). In the MPS group, several large and small hyperchromatic rounded muscle cells appeared (arrows), the abnormal fibers were aggregated together, and slightly inflammatory cells could be observed, showing short cracks and large gaps within the muscle fiber framework. (E) Light microscopy images of longitudinal sections of muscle fibers with H&E staining. In the control group, the muscle cells were tightly ordered. In the MPS group, the muscle cells showed continuously inflated and tapering fibers (arrows). H&E: hematoxylin and eosin; MPS: myofascial pain syndrome; MTRPs: myofascial trigger points; SEM: standard error of the mean; TB: taut band.

blotting to detect the expression of ERK and p-ERK. Total ERK expression was not affected by the injection of the ERK inhibitor U0126. ERK phosphorylation was downregulated

after injection of two different concentrations (0.2 and 1  $\mu\text{g}/\mu\text{l}$ ) of ERK inhibitor compared to that in the MPS + DMSO group (Fig. 4).

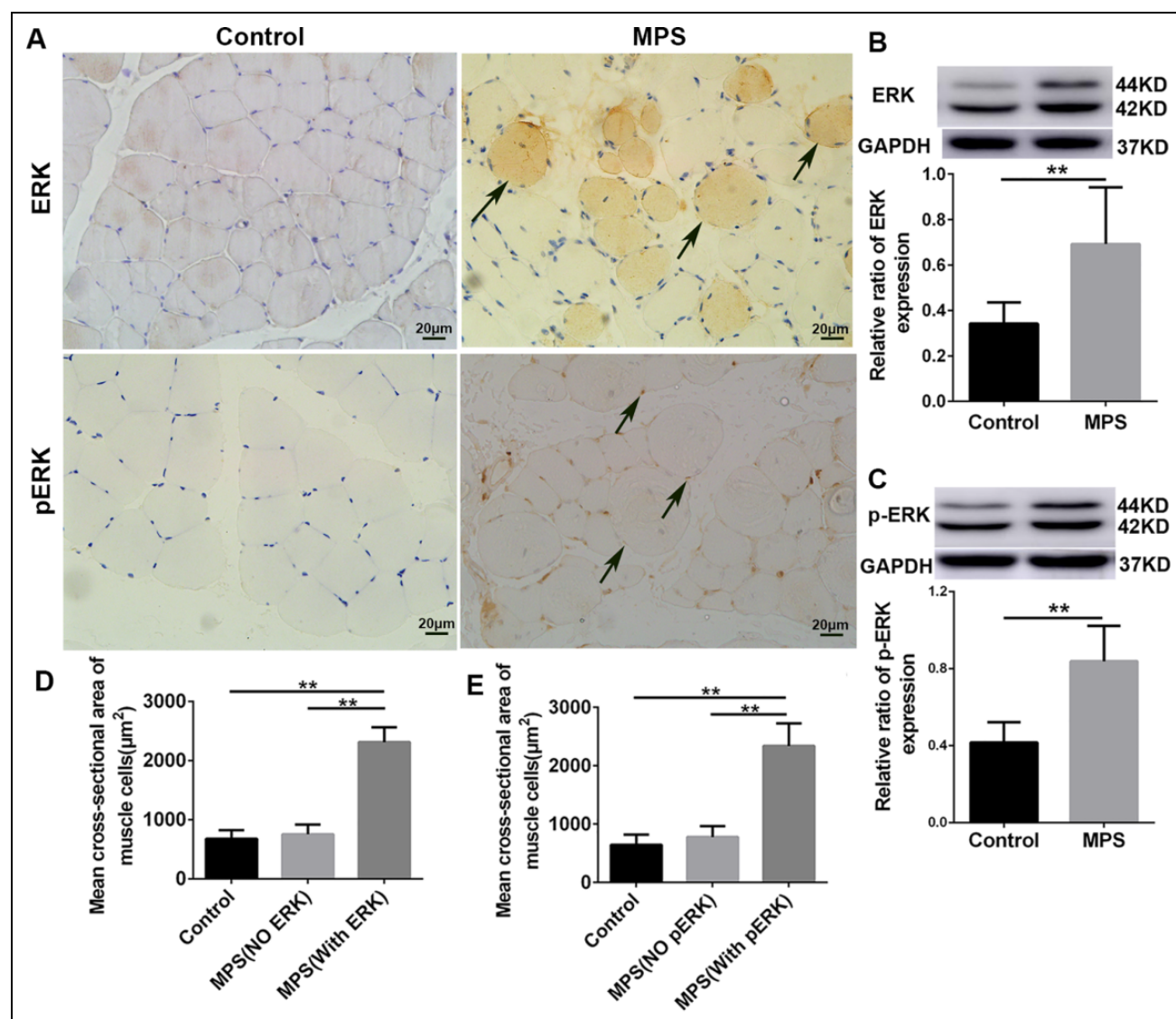


**Figure 3.** ERK and p-ERK expressions were increased in injured muscle fibers around MTrPs of the gastrocnemius muscle of SD rats. (A) Representative immunohistochemical staining of ERK and p-ERK protein expressions in injured muscle fibers around MTrPs of the gastrocnemius muscle. ERK was increased in the cytoplasm of large or small rounded muscle cells (arrows) in the MPS group. P-ERK was increased in the cell nuclei of muscle cells (arrows) in the MPS group. (B and C) Representative bands showing ERK and p-ERK protein expressions in the gastrocnemius muscle after modeling of the two groups. The quantitative data for both ERK and p-ERK protein expressions are represented by the means  $\pm$  SEMs ( $n = 6$ ) based on the band density normalized to that of GAPDH. The data were analyzed by *T*-tests. \* $P < 0.05$ , \*\* $P < 0.01$ . (D) Muscle cell cross-sectional area in the control group, MPS (no ERK) group, and MPS (with ERK) group. Data are presented as the mean  $\pm$  SEM ( $n = 3$ ). The data were analyzed using one-way ANOVA. \*\* $P < 0.01$ . (E) Muscle cell cross-sectional area in the control group, MPS (no p-ERK) group, and MPS (with p-ERK) group. Data are presented as the mean  $\pm$  SEM ( $n = 3$ ). The data were analyzed using one-way ANOVA. \*\* $P < 0.01$ . ANOVA: analysis of variance; GAPDH: glyceraldehyde 3-phosphate dehydrogenase; MPS: myofascial pain syndrome; MTrPs: myofascial trigger points; SD: Sprague–Dawley; SEM: standard error of the mean; TB: taut band.

### ERK Inhibitor Ameliorated Muscular Mechanical Hyperalgesia and Reduced the Cross-sectional Area in Muscle Cells

The mechanical pain threshold of rats was measured using a Randall-Selitto apparatus at 0.5, 1, 2, 3, 4, 5, 8, 12, 18, and 24 h after injection of different concentrations of ERK

inhibitor. In our preliminary experiment, no significant difference in behavior was noted between the Control + U1 group and the Control + DMSO group. In the MPS + U0.2 ( $n = 6$ ) and MPS + U1 ( $n = 6$ ) groups, MTrP administration of U0126 (one to three points) produced significant recovery of mechanical hyperalgesia compared with the MPS + DMSO group at 0.5, 1, 2, 3, 4, and 5 h after injection of

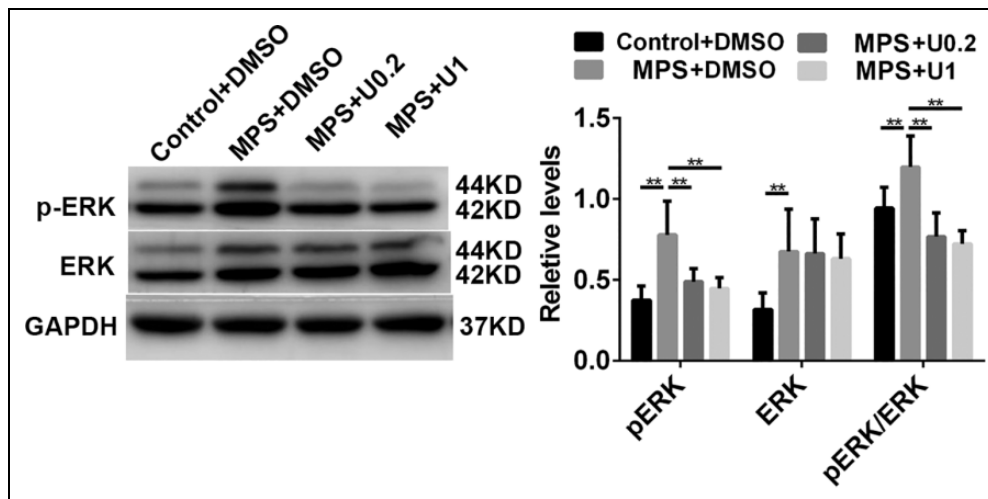


**Figure 4.** ERK inhibitor restrained the expression of p-ERK. Total ERK expression was not affected by the ERK inhibitor U0126 1 h after injection. ERK phosphorylation and pERK/ERK were significantly downregulated in the ERK inhibitor U0126 group at two different concentrations (0.2 and 1  $\mu\text{g}/\mu\text{l}$ ) 1 h after injection. Data are presented as the mean  $\pm$  SEM ( $n = 6$ ). The data were analyzed using one-way ANOVA. \* $P < 0.05$ , \*\* $P < 0.01$ . ANOVA: analysis of variance; SEM: standard error of the mean.

ERK inhibitor (Fig. 5A). As shown in Fig. 5B, the cross-sectional area of muscle cells in the MPS + DMSO group significantly increased (\*\* $P < 0.01$  compared with that in the Control + DMSO group). In contrast, the cross-sectional area of muscle cells in the MPS + U0.2 and MPS + U1 groups decreased (Fig. 5B; \* $P < 0.05$  compared with that in the MPS + DMSO group), indicating that the ERK inhibitor effectively relieves muscle contraction.

#### *MLCK is Potentially a Target of ERK Inhibitor Involved in Ameliorating Muscular Mechanical Hyperalgesia*

The relationship between ERK and MLCK was shown by the bioinformatics prediction performed by using the STRING database (Fig. 6A). MLCK and p-MLC expressions were significantly upregulated in the MPS group compared with the control group. MLCK and p-MLC expressions in injured muscle fibers around MTrPs were significantly downregulated in the MPS + U0.2 and MPS + U1 groups compared with the MPS + DMSO group (Fig. 6B).

#### **Discussion**

This is the first study demonstrating the role of ERK pathways in injured muscle fibers around MTrPs in a rat myofascial pain model. We found that ERK was significantly increased in injured muscle fibers, and injured muscle fibers are a typical morphological feature of MTrPs. MTrPs may be an important cause of recurrent attacks of chronic or regional pain syndrome, whereas other conditions can also cause the formation of MTrPs<sup>29</sup>. Given that MTrPs play a key role in the occurrence and persistence of MPS and are also the cause of central changes, we attempted to reveal a new mechanistic view at the skeletal muscle cell and molecular levels. The

three main objective criteria for detecting MTrP include electromyographic recording of LTRs, spontaneous electrical activity at multiple sites of activity in the MTrPs, and biopsies of MTrPs, which exhibit contraction nodes and large round muscle fibers<sup>3</sup>. To reduce the damage caused by repeated insertion of the fine needle electrode in TB muscle tissue, we did not utilize electromyography but ensured the accuracy of the positions by detecting twitch responses and histomorphology.

MTrPs are mainly composed of many abnormally contracted sarcomeres (injured muscle fibers). Some studies suggest that muscle contraction is caused by excessive release of acetylcholine, causing pain, and disrupting the underlying cycle may be an effective method to treat symptoms. Botox treatment is a method used to achieve this, but the current clinical use of botulinum treatment is controversial. Are there other contraction pathways in skeletal muscle cells? ERK/MLCK play important roles in smooth muscle contraction, so do they play an important role in regulating skeletal muscle contraction? U0126, a specific inhibitor of ERK, is currently used to study various factors, such as neuralgia and inflammatory pain; however, the possibility that U0126 plays a role in the central nervous system cannot be excluded. However, the anti-hyperalgesia effect of U0126 is more likely to be caused by inhibiting the ERK signaling pathway in peripheral nociceptors, which gradually weakens with the extension of the drug administration time. These results suggest that the inhibitory effect of U0126 on hyperalgesia may be achieved by inhibiting the ERK signaling pathway. Our data demonstrate that ERK is involved in hyperalgesia in rats. Therefore, we used the ERK-specific inhibitor U0126 to investigate the mechanism of ERK in myofascial pain.

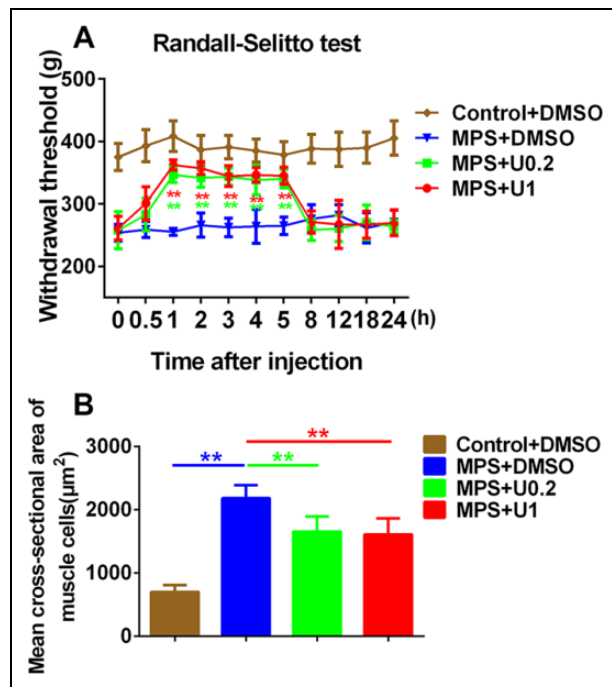


**Figure 5.** ERK inhibitor ameliorated muscular mechanical hyperalgesia and reduced the cross-sectional area of muscle cells. (A) Effects of different reagents on the mechanical pain threshold of rats. Mechanical pain threshold of rats measured using a Randall-Selitto apparatus at 0.5, 1, 2, 3, 4, 5, 8, 12, 18, and 24 h after injection of different concentrations of inhibitor. Data are presented as the mean  $\pm$  SEM ( $n = 6$ ). The data were analyzed using one-way ANOVA. Red \*\* indicates the MPS + U1 group versus the MPS + DMSO group, and green \*\* indicates the MPS + U0.2 group versus the MPS + DMSO group. \* $P < 0.05$ , \*\* $P < 0.01$ . (B) Muscle cell cross-sectional area in the control + DMSO group, MPS + DMSO group, MPS + U0.2 group, and MPS + U1 group. Data are presented as the mean  $\pm$  SEM ( $n = 6$ ). The data were analyzed using one-way ANOVA. \* $P < 0.05$ , \*\* $P < 0.01$ . ANOVA: analysis of variance; DMSO: dimethyl sulfoxide; MPS: myofascial pain syndrome; SEM: standard error of the mean.

Some studies have suggested that MTrPs are caused by muscle strain, muscle mechanical injury, or mental stress<sup>30</sup>. Improper posture in daily life and work, muscle contusion caused by direct external force and pulling caused by indirect external force, or insufficient blood supply to muscle cells caused by other means cause cell membrane damage, which serves as the initial event in muscle damage<sup>31,32</sup>. Increasing evidence has demonstrated that these causes of myofascial pain significantly affect ERK activation<sup>33,34</sup>. ERK is key to transmitting signals from surface receptors to the nucleus involved in cell proliferation and differentiation, cell morphology maintenance, and cytoskeleton construction and may play an important role in a series of myogenic reactions caused by muscle contraction<sup>35,36</sup>. According to our results, ERK may be the key molecule involved in the abnormal contraction of MTrPs caused by various mechanical factors. IHC and WB results showed

that ERK and p-ERK protein expressions in injured muscle fibers around MTrPs were significantly increased. Importantly, ERK is involved in the activation of many nuclear transcription factors to adapt the body to different external stimuli, including local tissue stress caused by muscle contraction<sup>37,38</sup>. Phosphorylated ERK1/2 (phospho-ERK1/2, p-ERK1/2) enters the nucleus mainly in the form of a homologous dimer via a nuclear localization sequence, and a small amount of p-ERK1/2 remains in the cytoplasm<sup>39</sup>. ERK1/2 may be involved in the adaptive changes in skeletal muscle during exercise or other contractile activities by activating related nuclear transcription factors, such as Myc, Elk-1, and c-Fos. In other experiments, such as those performed in vascular smooth muscle and some smooth muscle endothelial cells, ERK significantly affected MLCK expression<sup>20,40</sup>. In our experiment, MLCK protein expression in the MPS + DMSO group increased, and MLCK protein expression decreased after ERK inhibitor injection, indicating that ERK was the upstream factor driving the change in MLCK levels.

MLCK has been extensively studied in smooth muscle and its mechanism is relatively clear. However, its role in skeletal muscle has been rarely studied. Although  $Ca^{2+}$  binds to troponin, resulting in changes in troponin configuration that lead to subsequent muscle contraction and representing the main mechanism of skeletal muscle contraction, RLC is essential in regulating the development of muscle strength<sup>25</sup>. Increasing evidence shows that MLCK plays a major role in muscle fiber contraction<sup>26</sup>. RLC phosphorylation plays an important role in the enhancement of the strength of IIB-type muscle fibers<sup>41</sup>. In addition, studies have shown that single nucleotide polymorphisms in skMLCK are related to the vulnerability of human muscles to injury during strenuous activities<sup>42</sup>. RLC phosphorylation leads to biochemical memory affecting enhanced twitch force<sup>41</sup>, and this effect may produce an increased degree of contraction resulting in muscle damage<sup>23</sup>. Based on the above research results, the abnormal increases in MLCK and p-MLC proteins in skeletal muscle cells may lead to abnormal muscle contraction and the formation of abnormally contracted sarcomeres. In our study, after the injection of inhibitors, MLCK and p-MLC expressions were downregulated, and the cross-sectional area of large round muscle cells was decreased, indicating that MLCK was involved in the abnormal contraction mechanism of the sarcomere.

In our experiment, repeated blunt striking injury and eccentric exercise caused gastrocnemius hyperalgesia accompanied by the formation of injured muscle fibers, which is consistent with the characteristics of MTrPs. Simons' integrated hypothesis suggests that MTrPs are caused by muscle strain and muscle mechanical injury, which cause excessive acetylcholine release<sup>30</sup>. Excessive release of acetylcholine leads to muscle contraction and causes local blood circulation disorders, resulting in an insufficient energy supply to tissues. Tissues release

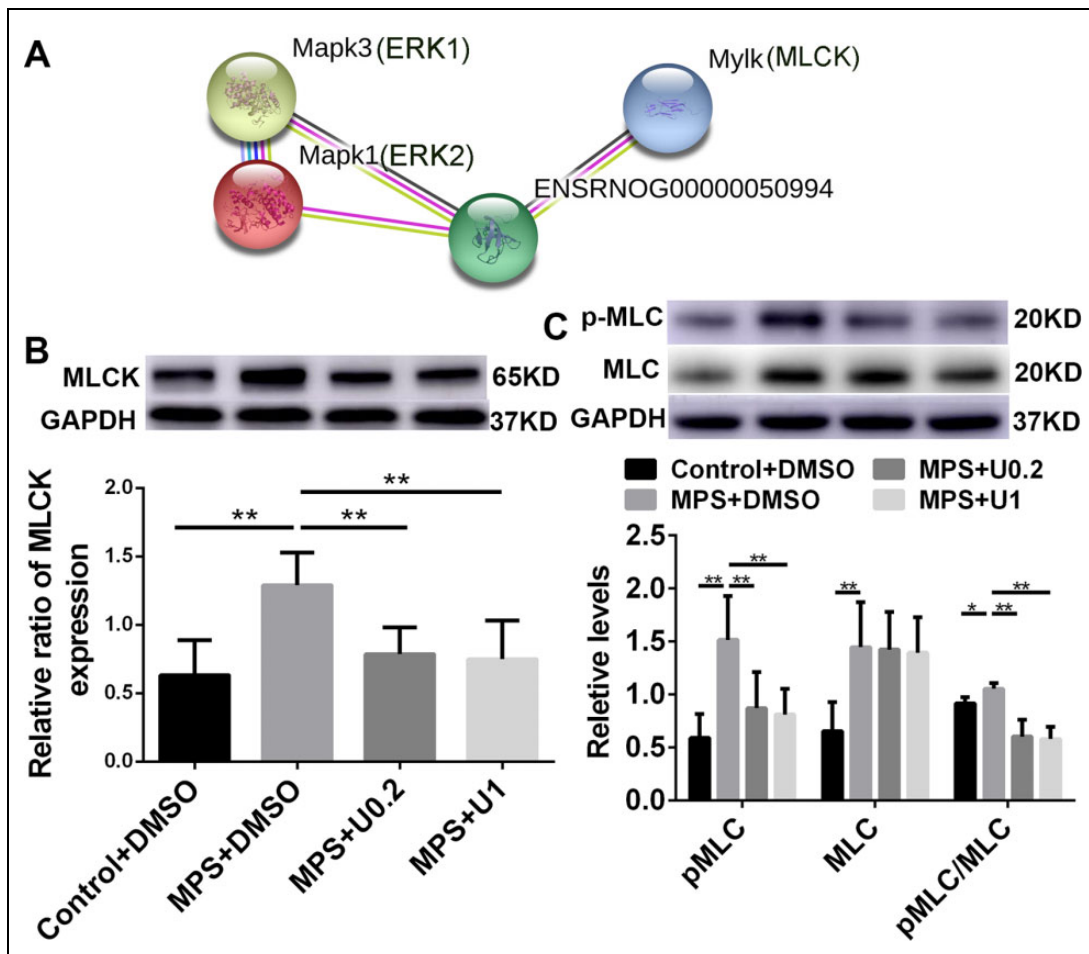


**Figure 6.** MLCK might be the target of the ERK inhibitor involved in ameliorating muscular mechanical hyperalgesia. (A) The relationship between ERK and MLCK was shown by bioinformatics prediction with the STRING database. (B) The expression of MLCK protein. MLCK expression was increased in the MPS group compared with that in the control group. MLCK expression was decreased in the ERK inhibitor group compared with that in the MPS group. Data are presented as the mean  $\pm$  SEM ( $n = 6$ ). The data were analyzed using one-way ANOVA.  $*P < 0.01$ . (C) The expression of p-MLC protein. p-MLC expression was increased in the MPS group compared with that in the control group. p-MLC expression was decreased in the ERK inhibitor group compared with that in the MPS group. Data are presented as the mean  $\pm$  SEM ( $n = 6$ ). The data were analyzed using one-way ANOVA.  $*P < 0.01$ . ANOVA: analysis of variance; MLCK: myosin light chain kinase; MPS: myofascial pain syndrome; SEM: standard error of the mean.

sensitive substances (ATP, BK, 5-HT, prostaglandins,  $K^+$ , etc.) that cause excitability of nociceptors, and peripheral nerve sensitization can lead to abnormal release of acetylcholine. Interestingly, no direct evidence of an increase in acetylcholine at MTrPs has been reported, and the clinical efficacy of Botox (a drug that inhibits the release of acetylcholine) in treating myofascial pain remains controversial. Our results further supported the integrated hypothesis of myofascial MTrPs. During skeletal muscle contraction, the increased concentration of  $Ca^{2+}$  in the cytoplasm can cause  $Ca^{2+}$  to bind to CaM, and then the  $Ca^{2+}$ /CaM complex binds to skMLCK, resulting in activation<sup>43</sup>, which increases the speed and strength of muscle contractions. When these changes exceed the regulatory capacity of the cell itself, cell damage occurs. Excessive activation of MLCK leads to more

energy consumption by muscle cells, which leads to an energy crisis in the local microenvironment. The persistent abnormal contraction leads to abnormal expansion of muscle fibers, an increase in the cross-sectional area, and compression of the peripheral blood vessels or nerves, resulting in further pain from ischemia or nerve compression. After we injected ERK inhibitor, we observed a reduction in hyperalgesia, which may be related to the reduction of the muscle fiber cross-sectional area.

The disadvantage of this experiment is that although we tried our best to obtain the muscle tissue from the MTrP, we could not precisely obtain the trigger point tissue due to the three-dimensional structure of the muscle tissue. Because the tissue we sampled may contain nontrigger point tissue, we can only study the trigger point and its surrounding injured

muscle fibers as a whole. We attempted to determine the causes of persistent muscle pain at the cellular and molecular levels from this perspective. How to precisely collect trigger point tissue and how trigger point tissue causes persistent muscle pain should be further studied.

In conclusion, repeated strikes and eccentric exercise caused chronic muscular mechanical hyperalgesia accompanied by muscle fiber injury. The present study demonstrated that ERK and p-ERK were more highly expressed in injured muscle fibers around MTrPs, leading to an increase in MLCK expression and abnormal contraction of the muscle fibers. This mechanism may be the cause of persistent muscle pain around MTrPs from contused gastrocnemius muscle in rats. This information may provide new ideas and targets for the treatment of patients with MPS at the cellular and molecular levels.

### Acknowledgments

We thank the Key Laboratory of Cardiovascular Remodeling and Function Research of Qilu Hospital for its help.

### Ethical Approval

All animal procedures used in this study were approved by the Ethics Committee of Shandong University, Shandong Province, China (reference number: KYLL-2014-027).

### Statement of Human and Animal Rights

All of the experimental procedures involving animals were conducted in accordance with Institutional Animal Care guidelines of Shandong University, China and approved by the Administration Committee of Experimental Animals, Shandong Province, China.

### Statement of Informed Consent

There are no human subjects involved in the study in this article, and informed consent is not applicable.

### Declaration of Conflicting Interests

The author(s) declared no potential conflicts of interest with respect to the research, authorship, and/or publication of this article.

### Funding

The author(s) disclosed receipt of the following financial support for the research, authorship, and/or publication of this article: This study was funded in part by the National Natural Science Foundation of China (No. 81672250) and the Fundamental Research Funds of Shandong University.

### ORCID iD

Yu-Chang Zhu  <https://orcid.org/0000-0003-1145-6866>

### References

- Fayaz A, Croft P, Langford RM, Donaldson LJ, Jones GT. Prevalence of chronic pain in the UK: a systematic review and meta-analysis of population studies. *BMJ Open*. 2016;6(6):e010364.
- de Souza JB, Grossmann E, Perissinotti DMN, de Oliveira Junior JO, da Fonseca PRB, Posso IP. Prevalence of chronic pain, treatments, perception, and interference on life activities: brazilian population-based survey. *Pain Res Manag*. 2017; 2017:4643830.
- Huang QM, Ye G, Zhao ZY, Lv JJ, Tang L. Myoelectrical activity and muscle morphology in a rat model of myofascial trigger points induced by blunt trauma to the vastus medialis. *Acupunct Med*. 2013, 31(1):65–73.
- Bordoni B, Sugumar K, Varacallo M. *Myofascial Pain*. Treasure Island (FL): StatPearls; 2020.
- Wheeler AH, Aaron GW. Muscle pain due to injury. *Curr Pain Headache R*. 2001;5(5):441–446.
- Cummings M, Baldry P. Regional myofascial pain: diagnosis and management. *Best Pract Res Clin Rheumatol*. 2007, 21(2): 367–387.
- Zhuang X, Tan S, Huang Q. Understanding of myofascial trigger points. *Chin Med J*. 2014, 127(24):4271–4277.
- Zhang H, Lu JJ, Huang QM, Liu L, Liu QG, Eric OA. Histopathological nature of myofascial trigger points at different stages of recovery from injury in a rat model. *Acupunct Med*. 2017, 35(6):445–451.
- Lv H, Li Z, Hu T, Wang Y, Wu J, Li Y. The shear wave elastic modulus and the increased nuclear factor kappa B (NF- $\kappa$ B/p65) and cyclooxygenase-2 (COX-2) expression in the area of myofascial trigger points activated in a rat model by blunt trauma to the vastus medialis. *J Biomech*. 2018, 66:44–50.
- Li LH, Huang QM, Barbero M, Liu L, Nguyen TT, Beretta-Piccoli M, Xu AL, Ji LJ. Quantitative proteomics analysis to identify biomarkers of chronic myofascial pain and therapeutic targets of dry needling in a rat model of myofascial trigger points. *J Pain Res*. 2019;12:283–298.
- Margalef R, Sisquella M, Bosque M, Romeu C, Mayoral O, Monterde S, Priego M, Guerra-Perez R, Ortiz N, Tomàs J, Santafe MM. Experimental myofascial trigger point creation in rodents. *J Appl Physiol*. 2019;126(1):160–169.
- Gerwin RD, Cagnie B, Petrovic M, Van Dorpe J, Calders P, De Meulemeester K. Foci of segmentally contracted sarcomeres in trapezius muscle biopsy specimens in myalgic and nonmyalgic human subjects: preliminary results. *Pain Med*. 2020;0(0):1–9.
- Cao L, Gao Y, Wu K, Li Y, Chen C, Yuan S. Sympathetic hyperinnervation in myofascial trigger points. *Med Hypotheses*. 2020;139:109633.
- Zhang M, Jin F, Zhu Y, Qi F. Peripheral FGFR1 Regulates Myofascial Pain in Rats via the PI3K/AKT Pathway. *Neuroscience*. 2020;436:1–10.
- Obata K, Noguchi K. MAPK activation in nociceptive neurons and pain hypersensitivity. *Life Sci*. 2004;74(21):2643–2653.
- Ji RR, Gereau RWt, Malcangio M, Strichartz GR. MAP kinase and pain. *Brain Res Rev*. 2009;60(1):135–148.
- Turjanski AG, Vaque JP, Gutkind JS. MAP kinases and the control of nuclear events. *Oncogene*. 2007;26(22):3240–3253.
- Tschumperlin DJ, Shively JD, Swartz MA, Silverman ES, Haley KJ, Raab G, Raab G, Drazen JM. Bronchial epithelial compression regulates MAP kinase signaling and HB-EGF-like growth factor expression. *Am J Physiol Lung Cell Mol Physiol*. 2002;282(5):L904–911.

19. Qu YJ, Jia L, Zhang X, Wei H, Yue SW. MAPK pathways are involved in neuropathic pain in rats with chronic compression of the dorsal root ganglion. *Evid Based Complement Alternat Med*. 2016;2016:6153215.
20. Tan J, Wang Y, Xia Y, Zhang N, Sun X, Yu T, Lin L. Melatonin protects the esophageal epithelial barrier by suppressing the transcription, expression and activity of myosin light chain kinase through ERK1/2 signal transduction. *Cell Physiol Biochem*. 2014;34(6):2117–2127.
21. Cheng X, Wan Y, Xu Y, Zhou Q, Wang Y, Zhu H. Melatonin alleviates myosin light chain kinase expression and activity via the mitogen-activated protein kinase pathway during atherosclerosis in rabbits. *Mol Med Rep*. 2015;11(1):99–104.
22. Kamm KE, Stull JT. Dedicated myosin light chain kinases with diverse cellular functions. *J Biol Chem*. 2001;276(7):4527–4530.
23. Childers MK, McDonald KS. Regulatory light chain phosphorylation increases eccentric contraction-induced injury in skinned fast-twitch fibers. *Muscle Nerve*. 2004;29(2):313–317.
24. Sweeney HL, Bowman BF, Stull JT. Myosin light chain phosphorylation in vertebrate striated muscle: regulation and function. *Am J Physiol*. 1993;264(5 Pt 1):C1085–1095.
25. Szczesna D, Zhao J, Jones M, Zhi G, Stull J, Potter JD. Phosphorylation of the regulatory light chains of myosin affects Ca<sup>2+</sup> sensitivity of skeletal muscle contraction. *J Appl Physiol*. 2002;92(4):1661–1670.
26. Zhi G, Ryder JW, Huang J, Ding P, Chen Y, Zhao Y, Kamm KE, Stull JT. Myosin light chain kinase and myosin phosphorylation effect frequency-dependent potentiation of skeletal muscle contraction. *Proc Natl Acad Sci U S A*. 2005;102(48):17519–17524.
27. Alvarez P, Green PG, Levine JD. Role for monocyte chemoattractant protein-1 in the induction of chronic muscle pain in the rat. *Pain*. 2014;155(6):1161–1167.
28. Alvarez P, Bogen O, Green PG, Levine JD. Nociceptor interleukin 10 receptor 1 is critical for muscle analgesia induced by repeated bouts of eccentric exercise in the rat. *Pain*. 2017;158(8):1481–1488.
29. Gerwin RD. Classification, epidemiology, and natural history of myofascial pain syndrome. *Curr Pain Headache Rep*. 2001;5(5):412–420.
30. Gerwin RD, Dommerholt J, Shah JP. An expansion of Simons' integrated hypothesis of trigger point formation. *Curr Pain Headache Rep*. 2004;8(6):468–475.
31. Armstrong RB, Warren GL, Warren JA. Mechanisms of exercise-induced muscle fibre injury. *Sports Med*. 1991;12(3):184–207.
32. Gissel H. The role of Ca<sup>2+</sup> in muscle cell damage. *Ann N Y Acad Sci*. 2005;1066:166–180.
33. Wretman C, Lionikas A, Widegren U, Lannergren J, Westerblad H, Henriksson J. Effects of concentric and eccentric contractions on phosphorylation of MAPK(erk1/2) and MAPK(p38) in isolated rat skeletal muscle. *J Physiol*. 2001;535(Pt 1):155–164.
34. Williamson D, Gallagher P, Harber M, Hollon C, Trappe S. Mitogen-activated protein kinase (MAPK) pathway activation: effects of age and acute exercise on human skeletal muscle. *J Physiol*. 2003;547(Pt 3):977–987.
35. Jones NC, Fedorov YV, Rosenthal RS, Olwin BB. ERK1/2 is required for myoblast proliferation but is dispensable for muscle gene expression and cell fusion. *J Cell Physiol*. 2001;186(1):104–115.
36. Adi S, Bin-Abbas B, Wu NY, Rosenthal SM. Early stimulation and late inhibition of extracellular signal-regulated kinase 1/2 phosphorylation by IGF-I: a potential mechanism mediating the switch in IGF-I action on skeletal muscle cell differentiation. *Endocrinology*. 2002;143(2):511–516.
37. Wojtaszewski JF, Lyngge J, Jakobsen AB, Goodyear LJ, Richter EA. Differential regulation of MAP kinase by contraction and insulin in skeletal muscle: metabolic implications. *Am J Physiol*. 1999;277(4):E724–E732.
38. Widegren U, Ryder JW, Zierath JR. Mitogen-activated protein kinase signal transduction in skeletal muscle: effects of exercise and muscle contraction. *Acta Physiol Scand*. 2001;172(3):227–238.
39. Roskoski R, Jr. ERK1/2 MAP kinases: structure, function, and regulation. *Pharmacol Res*. 2012;66(2):105–143.
40. Zhu HQ, Cheng XW, Xiao LL, Jiang ZK, Zhou Q, Gui SY, Wei W, Wang Y. Melatonin prevents oxidized low-density lipoprotein-induced increase of myosin light chain kinase activation and expression in HUVEC through ERK/MAPK signal transduction. *J Pineal Res*. 2008;45(3):328–334.
41. Ryder JW, Lau KS, Kamm KE, Stull JT. Enhanced skeletal muscle contraction with myosin light chain phosphorylation by a calmodulin-sensing kinase. *J Biol Chem*. 2007;282(28):20447–20454.
42. Clarkson PM, Hoffman EP, Zambraski E, Gordish-Dressman H, Kearns A, Hubal M, Harmon B, Devaney JM. ACTN3 and MLCK genotype associations with exertional muscle damage. *J Appl Physiol*. 2005;99(2):564–569.
43. Robertson SP, Johnson JD, Potter JD. The time-course of Ca<sup>2+</sup> exchange with calmodulin, troponin, parvalbumin, and myosin in response to transient increases in Ca<sup>2+</sup>. *Biophys J*. 1981;34(3):559–569.